International Journal of
Thermal Energy and Applications
Vol. 1: Issue 1
www.journalspub.com

CFD Applied to Fluid Flow Due to Motion of Lid Inside a Cavity

[1]Venkatshivasaivivek Attaluri*, [1]Parth N. Solanki, [1]Parth G. Patel, [1]Jatin D. Gami, [1]Nirvish P. Patel
[1]Student, Department of Mechanical Engineering, School Engineering and Technology, Navrachana University, Bhayli, Vadodara, Gujarat, India

ABSTRACT
A complete analysis of a lid-driven cavity is done using finite difference method of computational fluid dynamics. This analysis is applied to the transient Navier–Stokes equations in two dimensions as well as continuity equations in two dimensions. The results obtained from the present analysis give information on behavior of fluid at different values of the Reynolds number.

Keywords: *computational fluid dynamics, Navier–Stokes equations, Reynolds number*

***Corresponding Author**
E-mail: vivekattaluri3@gmail.com

INTRODUCTION
The lid-driven cavity problem has long been used as a test or validation case for new codes or new solution methods. The problem geometry is simple and two-dimensional (2D), and the boundary conditions are also simple. Simulations can also be done at various aspect ratios, and it can also be done with the lid replaced with a moving fluid. This problem has been solved as both a laminar flow and a turbulent flow, and many different numerical techniques have been used to compute these solutions. Since this case has been solved many times, there is a great deal of data to compare with. We are applying transient finite difference method (FDM) to Navier–Strokes equation. We have converted the unsteady Navier–Stokes equation into unsteady finite difference equation. We are then going to run the equations in a software and get the results. This work has been done before using the finite volume method using Ansys software. This would provide us some results to compare with. The data would be compared with the existing results which have been verified and an operating domain would be set in which the method would work. Once the software analysis gives some prominent results which seem to match the physical flow, then this method can be further used to predict different flows on different surfaces and different shape of cavities. These predictions can be achieved by changing the boundary conditions or by changing the shape or size of the boundary wall of the cavity.

REVIEW OF LITERATURE
A numerical work is performed to analyze combined convection heat transfer in fluid flow [1], and a finite volume technique is presented for the numerical solution of steady laminar flow of Oldroyd-B fluid in a lid-driven square cavity over a wide range of Reynolds and Weissenberg

numbers [2]. The effect of a variable spatial magnetic field on ferro-nanofluid flow and heat transfer in a double-sided lid-driven enclosure with a sinusoidal hot wall is investigated [3]. A study of a convergent and highly accurate mixed finite element technique to model the effect of fluid elasticity on the flow kinematics and the stress distribution in lid-driven cavity flow has been used [4]. Mixed convection heat transfer in a lid-driven cavity along with a heated circular hollow cylinder positioned at the center of the cavity has been analyzed numerically [5]. Improvements to a finite difference code, REBUFFS, have made possible the first completely successful simulation of the 3D lid-driven cavity flow [6], analyzing the OpenMP performances in order to simulate the lid-driven cavity flow using lattice Boltzmann method (LBM) [7]. Analyses of laminar mixed convection and entropy generation in a cubic lid-driven cavity have been performed numerically [8]. Stereo imaging methods are used to measure the positions of solid spherical particles suspended in a viscous liquid and enclosed in a transparent cubic cavity [9]. The problem of the time-dependent laminar incompressible flow motion within parallelepipedic cavities in which one wall moves with uniform velocity after an impulsive start using a particle-streak and a dye emission technique [10]. A finite difference scheme to compute steady-state solutions of the regularized 13 moment (R13) equations of rarefied gas dynamics [11], and 3D numerical simulations of fluid flow and heat transfer in a lid-driven cavity filled with a stably stratified fluid have been performed to study the effect of a sliding lid on the flow and thermal structures in a shallow cavity [12–14]. . A finite volume technique is done for the numerical solution of steady laminar flow of Oldroyd-B fluid in a lid-driven square cavity over a wide range of Reynolds and Weissenberg numbers [2]. A study of a convergent and highly accurate mixed finite element technique to model the effect of fluid elasticity on the flow kinematics and the stress distribution in lid-driven cavity flow has been used. In the numerical investigations, the corner singularities have been treated by incorporating a controlled amount of leakage which allows the computation of fully elastic mesh-converged solutions [4]. Numerical analysis of a mixed convection heat transfer in a lid-driven cavity along with a heated circular hollow cylinder positioned at the center of the cavity has been performed [5]. The effects of Prandtl number on the flow structure and heat transfer in the cavity are studied for laminar ranges of Re and Gr [15]. Various calculations through different methods and study on the effect of solid volume fraction, Rayleigh number and Reynolds number on the flow pattern and heat characteristics were investigated. Comes as positive effect on heat transfer enhancement [16]. Various numerical simulations of mixed convection flows in a square lid-driven cavity partially heated from below using Cu–water, Ag–water, Al_2O_3–water and TiO_2–water nanofluid were studied here, and FDM was employed for the solution of the present problem [17].

METHODOLOGY

Navier–Stokes Equation

It is a partial differential equation that describes the flow of incompressible, viscous flow.

A viscous flow is one where the transport phenomena of friction, thermal conduction, and/or mass diffusion are included. These transport phenomena are dissipative; they always increase the entropy of the flow.

$$\rho\left(\frac{\partial u}{\partial t}+u\frac{\partial u}{\partial x}+v\frac{\partial u}{\partial y}+w\frac{\partial u}{\partial z}\right)=-\frac{\partial p}{\partial x}+\mu\left(\frac{\partial^2 u}{\partial x^2}+\frac{\partial^2 u}{\partial y^2}+\frac{\partial^2 u}{\partial z^2}\right)+\rho g_x$$
$$\rho\left(\frac{\partial v}{\partial t}+u\frac{\partial v}{\partial x}+v\frac{\partial v}{\partial y}+w\frac{\partial v}{\partial z}\right)=-\frac{\partial p}{\partial y}+\mu\left(\frac{\partial^2 v}{\partial x^2}+\frac{\partial^2 v}{\partial y^2}+\frac{\partial^2 v}{\partial z^2}\right)+\rho g_y$$

The advantage of using a time-dependent Navier–Stokes approach is its inherent ability to evolve to the correct steady-state solution. The momentum equations for a viscous flow were identified as the *Navier–Stokes equations.* However, in the modern CFO literature, this terminology has been expanded to include the *entire system* of flow equations for the solution of a viscous flow continuity and energy as well as momentum. **Navier–Stokes equation**, in fluid_mechanics, is a partial differential equation that describes the flow of incompressible fluids. The equation is a generalization of the equation devised by Swiss mathematician, Leonhard Euler, in the 18th century to describe the flow of incompressible and frictionless fluids. In 1821, French engineer, Claude-Louis Navier, introduced the element of viscosity (friction) for more realistic and vastly more difficult problem of viscous fluids. Throughout the middle of the 19th century, the British physicist and mathematician, Sir George Gabriel Stokes, improved on this work, though complete solutions were obtained only for the case of simple 2D flows. The complex vortices and turbulence, or chaos, that occur in 3D fluid (including gas) flows as velocities increase, have proven intractable to any but approximate numerical analysis methods.

Conservation of Momentum

The momentum equation is a statement of Newton’s second law and relates the sum of the forces acting on an element of fluid to its acceleration or rate of change of momentum.

Newton’s 2nd law can be written as follows:
The rate of change of momentum of a body is equal to the resultant force acting on the body and takes place in the direction of the force.

Newton's second law, expressed above, when applied to the moving fluid element in Figure 1 says that the net force on the fluid element equals its mass times the acceleration of the element. This is a vector relation, and hence can be split into three scalar relations along the *x*-, *y*-, and *z*-axes. This type of analysis results into the momentum equations as follows:

$$\rho\frac{Du}{Dt}=-\frac{\partial p}{\partial x}+\frac{\partial \tau_{xx}}{\partial x}+\frac{\partial \tau_{yx}}{\partial y}+\frac{\partial \tau_{zx}}{\partial z}+\rho f_x$$
$$\rho\frac{Dv}{Dt}=-\frac{\partial p}{\partial y}+\frac{\partial \tau_{xy}}{\partial x}+\frac{\partial \tau_{yy}}{\partial y}+\frac{\partial \tau_{zy}}{\partial z}+\rho f_y$$
$$\rho\frac{Dw}{Dt}=-\frac{\partial p}{\partial z}+\frac{\partial \tau_{xz}}{\partial x}+\frac{\partial \tau_{yz}}{\partial y}+\frac{\partial \tau_{zz}}{\partial z}+\rho f_z$$

Continuity Equation

A **continuity equation** in physics is an equation that describes the transport of some quantity. It is particularly simple and powerful when applied to a conserved quantity, but it can be generalized to apply to any extensive quantity. Since mass, energy, momentum, electric charge and other natural quantities are conserved under their respective appropriate conditions, a variety of physical phenomena may be described using continuity equations.

Continuity equations are a stronger, local form of conservation laws. For example, a weak version of the law of conservation of energy states that energy can neither be created nor destroyed – i.e., the total amount of energy in the universe is fixed. This statement does not rule out the possibility that a quantity of energy could disappear from one point while simultaneously appearing at another point.

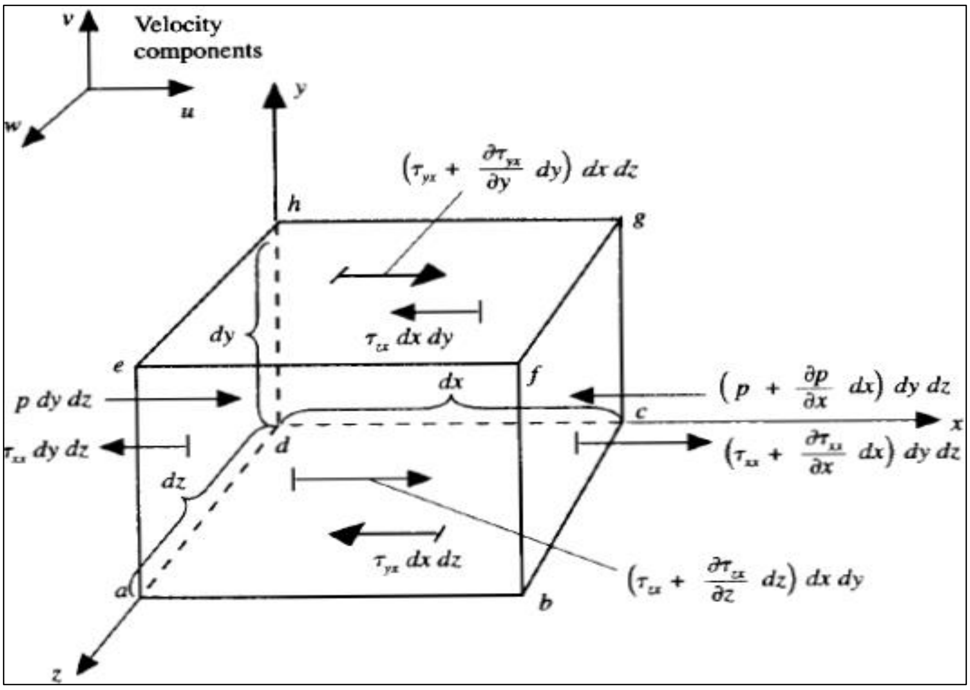

Fig. 1. *Newton's second law: when applied to the moving fluid element.*

A stronger statement is that energy is *locally* conserved: energy can neither be created nor destroyed, *nor* can it "teleport" from one place to another – it can only move by a continuous flow. A continuity equation is the mathematical way to express this kind of statement. For example, the continuity equation for electric charge states that the amount of electric charge in any volume of space can only change by the amount of electric current flowing into or out of that volume through its boundaries.

The integral form of the continuity equation states that:

- The amount of q in a region increases when additional q flows inward through the surface of the region, and decreases when it flows outward;
- The amount of q in a region increases when new q is created inside the region, and decreases when q is destroyed;
- Apart from these two processes, there is *no other way* for the amount of q in a region to change.

Mathematically, the integral form of the continuity equation expressing the rate of increase of q within a volume V is $\frac{dq}{dt} + \oiint_S \; j \cdot dS = \sum$, where

- S is any imaginary closed surface, that encloses a volume V,
- $\oiint S\, d\mathbf{S}$ denotes a surface integral over that closed surface,
- q is the total amount of the quantity in the volume V,
- $\mathbf{j}$ is the flux of q,
- t is time.

By the divergence theorem, a general continuity equation can also be written in a "differential form":

$$\frac{\partial p}{\partial t} + \nabla \cdot \boldsymbol{j} = \sigma$$

where

- $\nabla\cdot$ is divergence,
- ρ is the amount of the quantity q per unit volume,
- $\mathbf{j}$ is the flux of q,
- t is time,
- σ is the generation of q per unit volume per unit time. Terms that generate q (i.e., $\sigma > 0$) or remove q (i.e., $\sigma < 0$) are referred to as a "sources" and "sinks", respectively.

Finite Difference Method

FDMs are numerical methods for solving differential equations by approximating them with difference equations, in which finite differences approximate the derivatives. FDMs are the dominant approach to numerical solutions of partial differential equations. FDMs are thus discretization methods.

- First, a tailor series expansion is created of the function whose derivatives are to be approximated:

$$f(x_0+h)=f(x_0)+\frac{f'(x_0)}{1!}h+\frac{f^{(2)}(x_0)}{2!}h^2+\cdots+\frac{f^{(n)}(x_0)}{n!}h^n+R_n(x)$$

- Then, taking $x = a$, dividing by h and considering the remainder term is sufficiently small, we get:

$$f'(a)\approx\frac{f(a+h)-f(a)}{h}.$$

Error in Finite Differential Method

- The error in FDM is defined as the difference in the approximate and exact analytical methods.
- To use an FDM to approximate the solution to a problem, one must first discretize the problem's domain. This is usually done by dividing the domain into a uniform grid.
- FDMs produce sets of discrete numerical approximations to the derivative, often in a "time-stepping" manner.
- The error in the method can be reduced by expanding the tailor series to a higher order.

DERIVATION

Navier–Strokes equation in 2D:

$$\frac{\partial u}{\partial t}+u\frac{\partial u}{\partial x}+\vartheta\frac{\partial u}{\partial y}+W\frac{\partial u}{\partial z}=\frac{-1}{\rho}\frac{\partial p}{\partial x}+\frac{\mu}{\rho}\left(\frac{\partial^2 u}{\partial x^2}+\frac{\partial^2 u}{\partial y^2}+\frac{\partial^2 u}{\partial z^2}\right)+g \qquad (1)$$

$$\frac{\partial \vartheta}{\partial t}+u\frac{\partial \vartheta}{\partial x}+\vartheta\frac{\partial \vartheta}{\partial y}+W\frac{\partial \vartheta}{\partial z}=\frac{-1}{\rho}\frac{\partial p}{\partial y}+\frac{\mu}{\rho}\left(\frac{\partial^2 \vartheta}{\partial x^2}+\frac{\partial^2 \vartheta}{\partial y^2}+\frac{\partial^2 \vartheta}{\partial z^2}\right)+g \qquad (2)$$

The above terms are for incompressible 2D Navier–Stroke equation. The following equation is incompressible flow equation:

$$\frac{\partial u}{\partial x}+\frac{\partial \vartheta}{\partial y}=0\ (\because \nabla.\vec{v}=0) \qquad (3)\ \because \nabla.\vec{v}$$

In order to simplify the discretization process, steam function–vorticity method is easy and suitable at elementary level. This is accompanied by finite difference description of formatted equations.

The simplicity of converting u, ϑ velocities in stream function is actually converting two variables into one variable. Hence the computational complexity of calculating variables gets reduced.

Hence, $u=\frac{\partial \Psi}{\partial y}$ and $\vartheta=-\frac{\partial \Psi}{\partial x}$, according to the definition of stream function. (4)

From the definition of vorticity,

$$\frac{\partial \vartheta}{\partial x} - \frac{\partial u}{\partial y} = \omega \tag{5}$$

Now, differentiating Equations (1) and (2) with respect to "*y*" and "*x*", respectively, we get

$$\frac{\partial^2 u}{\partial t \partial y}+\frac{\partial u \partial u}{\partial x \partial y}+\mathrm{u}\frac{\partial^2 u}{\partial y \partial x}+\frac{\partial u}{\partial y}\frac{\partial \vartheta}{\partial y}+\vartheta\,\frac{\partial^2 u}{\partial y^2}=\frac{-1}{\rho}\,\frac{\partial p}{\partial u \partial x}+\frac{\mu}{\rho}\left(\frac{\partial^3 y}{\partial y \partial x^2}+\frac{\partial^3 y}{\partial y^3}\right) \tag{6}$$

$$\frac{\partial^2 y}{\partial t \partial x}+\frac{\partial \vartheta}{\partial x}\frac{\partial u}{\partial x}+\frac{\partial \vartheta}{\partial y}\frac{\partial \vartheta}{\partial x}+\mathrm{u}\frac{\partial^2 y}{\partial x^2}+\vartheta\,\frac{\partial^2 y}{\partial y \partial x}=\frac{-1}{\rho}\,\frac{\partial^2 y}{\partial y \partial x}+\frac{\mu}{\rho}\left(\frac{\partial^3 u}{\partial x^3}+\frac{\partial^3 \vartheta}{\partial y^2 \partial x}\right) \tag{7}$$

From Equations (6) and (7),

$$\frac{\partial^2 y}{\partial t \partial y}-\frac{\partial^2 \vartheta}{\partial t \partial x}+u\left(\frac{\partial^2 u}{\partial y \partial x}-\frac{\partial^2 \vartheta}{\partial x^2}\right)+\vartheta\left(\frac{\partial^2 u}{\partial y^2}-\frac{\partial^2 \vartheta}{\partial y \partial x}\right)+\frac{\partial u}{\partial y}\left(\frac{\partial \vartheta}{\partial y}+\frac{\partial u}{\partial x}\right)-\frac{\partial \vartheta}{\partial x}\left(\frac{\partial u}{\partial x}+\frac{\partial \vartheta}{\partial y}\right)=\frac{\mu}{\rho}\left(-\frac{\partial^3 \vartheta}{\partial x^3}+\frac{\partial^3 u}{\partial y \partial x^2}+\frac{\partial^3 u}{\partial y^3}-\frac{\partial^3 \vartheta}{\partial x \partial y^2}\right) \tag{8}$$

By applying this, Equation (8) gets reduced to vorticity equation as follows:

$$\frac{\partial \omega}{\partial t}+u\,\frac{\partial \omega}{\partial x}+\vartheta\,\frac{\partial \omega}{\partial y}=-\frac{\mu}{\rho}\left(\frac{\partial^2 \omega}{\partial x^2}+\frac{\partial^2 \omega}{\partial y^2}\right) \tag{9}$$

Hence, Equation (9) is now dimensional governing equation.
Converting Equation (9) into dimensionless equation,

let $\Omega = \frac{\omega h}{v_f}$,

$$X = \frac{x}{h}, Y = \frac{y}{h}, U = \frac{u}{v_f}; V = \frac{\vartheta}{v_f}; \tag{10}$$

$T = \frac{t v_f}{h}$; Re=Reynolds number = $\frac{\rho v_f h}{\mu}$.

Substituting Equation (10) in Equation (9), we get

$$\frac{\frac{\Omega v_f}{h}}{\frac{\partial T h}{v_f}}+\left(U v_f\right)\frac{\partial\left(\frac{\Omega v_f}{h}\right)}{\partial (Xh)}+\left(v v_f\right)\frac{\partial\left(\frac{\Omega v_f}{h}\right)}{\partial (Yh)}=\frac{\mu}{\rho}\left[\frac{\frac{\partial^2 \Omega v_f}{h}}{\partial (Yh)^2}+\frac{\partial^2\left(\frac{\Omega v_f}{h}\right)}{\partial (Xh)^2}\right] \tag{11}$$

$$\frac{\partial \Omega}{\partial T}+U\,\frac{\partial \Omega}{\partial X}+\vartheta\,\frac{\partial \Omega}{\partial Y}=\frac{1}{Re}\left(\frac{\partial^2 \Omega}{\partial Y^2}+\frac{\partial^2 \Omega}{\partial X^2}\right) \tag{12}$$

The above equation is now dimensionless governing differential equation.
Since, central difference gives us

$$\frac{\Omega_{ij}^{n+1}-\Omega_{ij}^{n}}{\Delta T}+\frac{U_{i+1,j}^{n}\Omega_{i+1,j}^{n}-U_{i-1,j}^{n}\Omega_{i-1,j}^{n}}{2\Delta X}+\frac{V_{i,j+1}^{n}\Omega_{i,j+1}^{n}-V_{i,j-1}^{n}\Omega_{i,j-1}^{n}}{2\Delta Y}=\frac{1}{Re}\left(\frac{\Omega_{i+1,j}^{n}-2\Omega_{i,j}^{n}+\Omega_{i-1,j}^{n}}{(\Delta X)^2}+\frac{\Omega_{i,j+1}^{n}-2\Omega_{i,j}^{n}+\Omega_{i,j-1}^{n}}{(\Delta Y)^2}\right) \tag{13}$$

Also, we had $\frac{\partial u}{\partial x} + \frac{\partial \vartheta}{\partial y} = 0$ (incompressible equation) (14)

Using stream function equation,

$$\frac{\partial^2 \Psi}{\partial x^2} + \frac{\partial^2 \Psi}{\partial y^2} = -\omega \tag{15}$$

Using $\Psi = \frac{\Psi}{v_f h}$ non-dimensional,

$$\frac{\partial^2 y}{\partial x^2} + \frac{\partial^2 y}{\partial y^2} = -\Omega \tag{16}$$

The discretization of Equation (16) is given as follows:

$$\frac{\Psi^n_{i+1,j} + \Psi^n_{i-1,j} - 2\Psi^n_{i,j}}{(\Delta x)^2} + \frac{\Psi^n_{i,j+1} + \Psi^n_{i,j-1} - 2\Psi^n_{i,j}}{(\Delta y)^2} = -\Omega^n_{i,j} \tag{17}$$

Once the equations are discretized, the next step is the application of boundary condition.

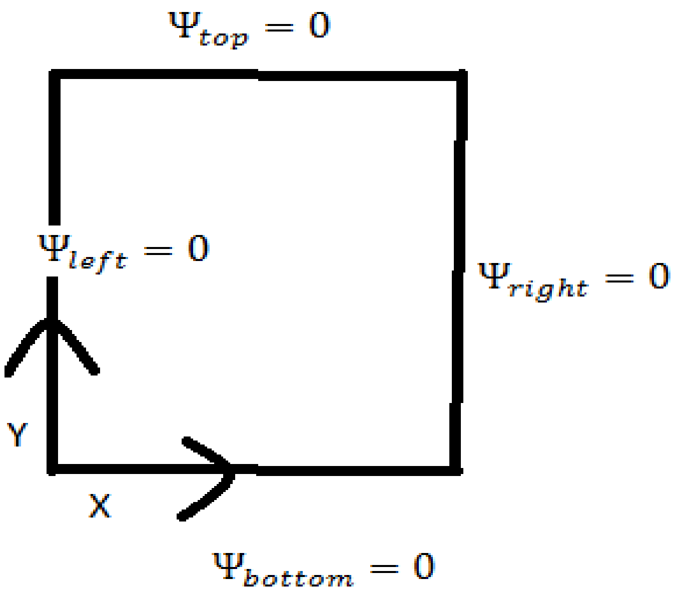

The top has x-direction dimensional velocity equal to unity, but since we are dealing with stream functions, the value of $\Psi = 0$ at all boundary conditions. From boundary conditions, using Equation (17), we can write Ω in terms of Ψ.

Rewriting Equation (17),

$$-\Omega^n_{i,j} = \frac{\Psi^n_{i,j+1} + \Psi^n_{i,j-1} - 2\Psi^n_{i,j}}{(\Delta Y)^2} + \frac{\Psi^n_{i+1,j} + \Psi^n_{i+1,j} - 2\Psi^n_{i,j}}{(\Delta X)^2} \tag{18}$$

For left, i = 1 in Equation (18), and $j = j$ and (remains same):

$\therefore$ $\Psi_{left} = 0$ becomes $\Psi^n_{i,j} = 0$

$I + 1 = 2$, $i - 1 = 0$ $\quad$ $j + 1 = j + 1$ (remains same)

∴ For left, Equation (18) becomes

$$\Omega^n_{i,j} = \frac{-\Psi^n_{0,j} - \Psi^n_{2,j}}{(\Delta x)^2} \tag{19}$$

We know that $\vartheta = 0$ (vertical velocity=0) for left,

$\frac{\partial \Psi}{\partial x} = 0$ ∴ writing in central difference scheme, (20)

$$\frac{\Psi^n_{2,j} - \Psi^n_{0,j}}{2\Delta X} = 0, j \tag{21}$$

$$\Psi^n_{0,j} = \Psi^n_{2,j} \tag{22}$$

Putting Equation (22) in Equation (19), $\Omega^n_{1,j} = \frac{-2\Psi^n_{2,j}}{(\Delta X)^2}$ (23)

Similarly, for right side and bottom side,

$$\Omega^n_{i.j} = \frac{-2\Psi^n_{i-1+j}}{(\Delta X)^2} \tag{24}$$

$$\Omega^n_{i.1} = \frac{-2\Psi^n_{i,2}}{(\Delta Y)^2} \tag{25}$$

For top side,

$$\Omega^n_{i+j} = -\left[\frac{-\Psi^n_{i,j-1} + \Psi^n_{i,j+1}}{(\Delta Y)^2}\right] \tag{26}$$

From the definition of stream function, in non-dimensional form for top side,

$$UV_f = \frac{\partial \Psi V_f h}{\partial Y h} \tag{27}$$

For top, $\Psi^n_{i,j+1}$ does not exist (everything is non-dimensional);

$$\therefore \text{ we use } U = \frac{\partial \Psi}{\partial Y} \tag{28}$$

∴ central difference scheme on Equation (28)

$$\Psi^n_{i,j+1} - \Psi^n_{i,j-1} = U\Delta Y \tag{29}$$

$$\Psi^n_{i,j+1} = U\Delta Y + \Psi^n_{i,j-1} \tag{30}$$

Put (30) in (26) to get $\Psi_{i.j+1}$, *U* is *x*-directional non-dimensional velocity

In order to get non-dimensional *X* and *Y* velocities, we use central difference scheme:

$$U^n_{i,j} = \frac{\Psi^n_{i,j+1} - \Psi^n_{i,j-1}}{2\Delta Y}\ ;\ V^n_{i,j} = -\frac{\Psi^n_{i+1,j} - \Psi^n_{i-1,j}}{2\Delta X}$$

RESULTS

The following results (Figures 2–13) were obtained for different values of Reynolds number. It can be easily be seen that the vorticity increases with the increase in Reynolds number.

Re = 1000

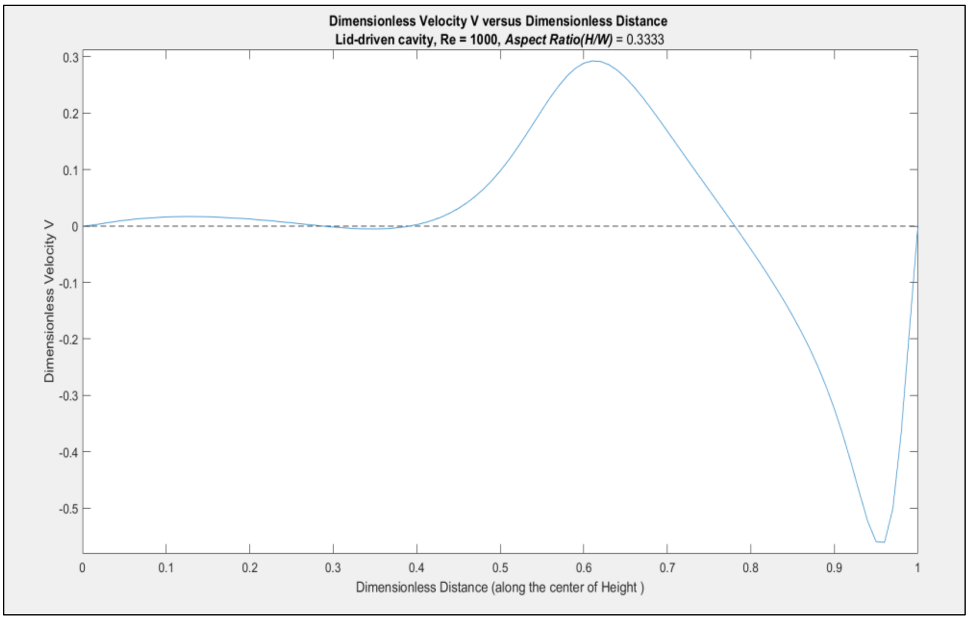

Fig. 2. *Simulation result for Re = 1000.*

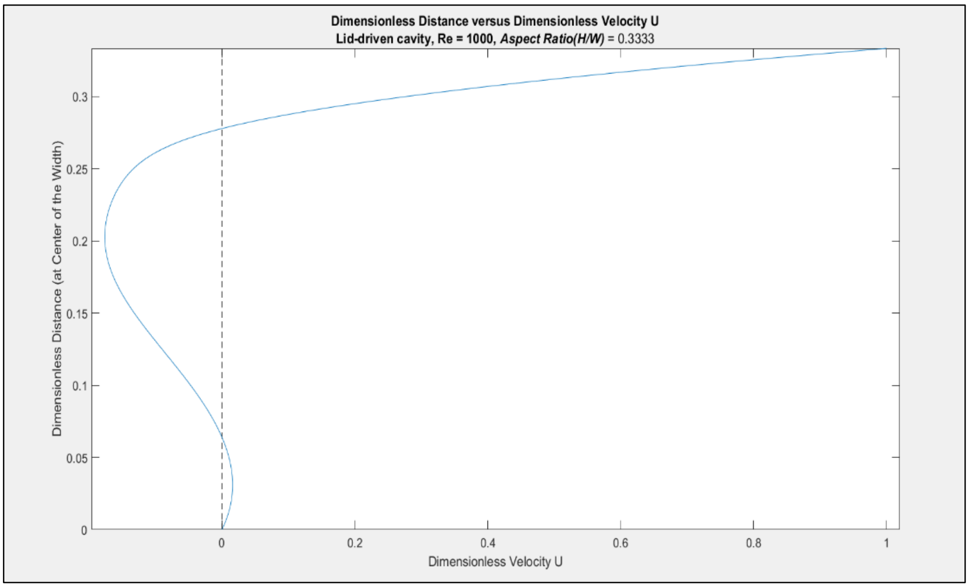

Fig. 3. *Simulation result for Re = 1000.*

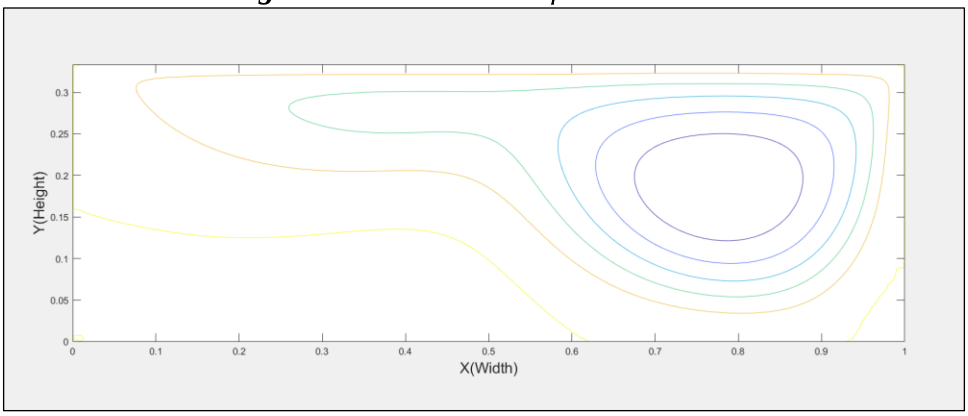

Fig. 4. *Simulation result for Re = 1000.*

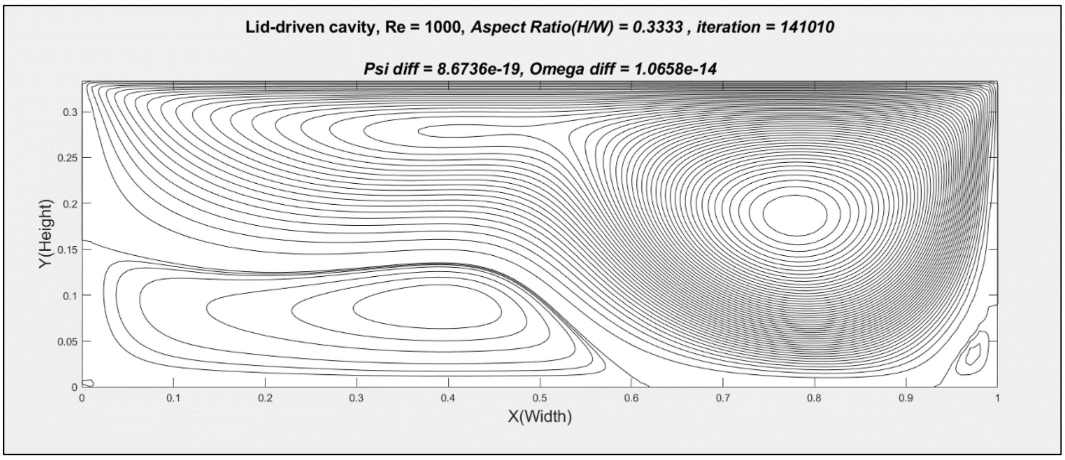

Fig. 5. *Simulation result for Re = 1000.*

Re = 750

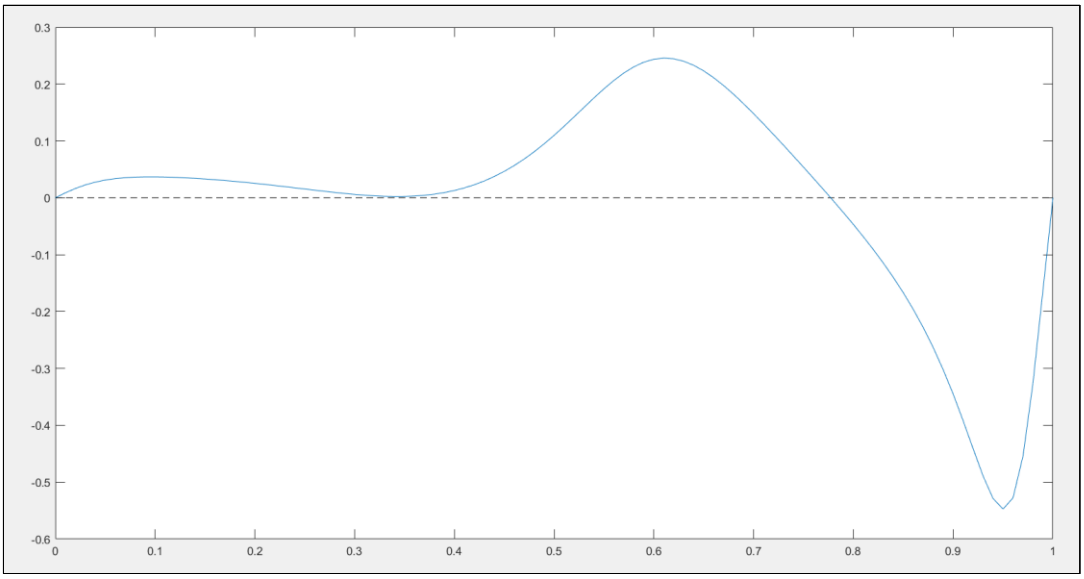

Fig. 6. *Simulation result for Re = 750.*

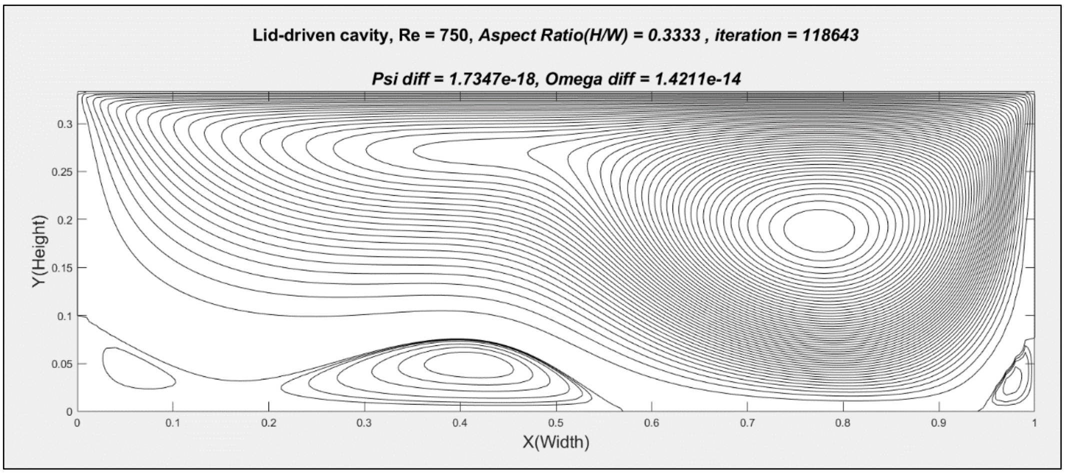

Fig. 7. *Simulation result for Re = 750.*

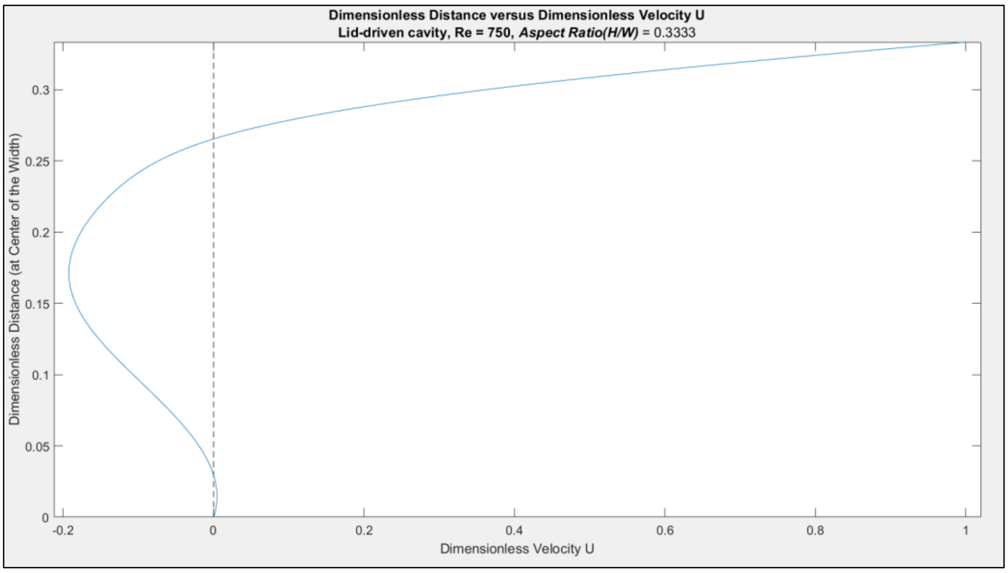

Fig. 8. *Simulation result for Re = 750.*

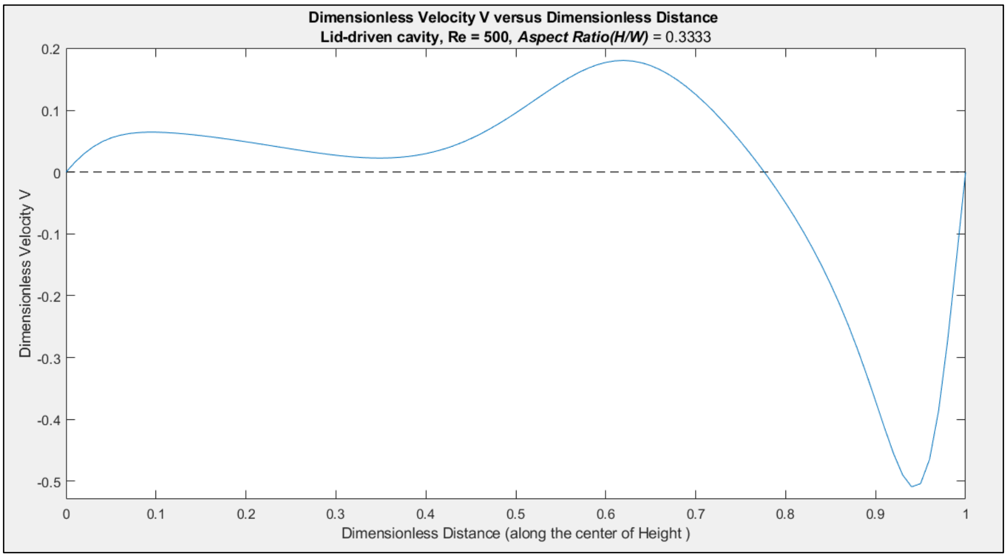

Fig. 9. *Simulation result for Re = 750.*

Re = 500

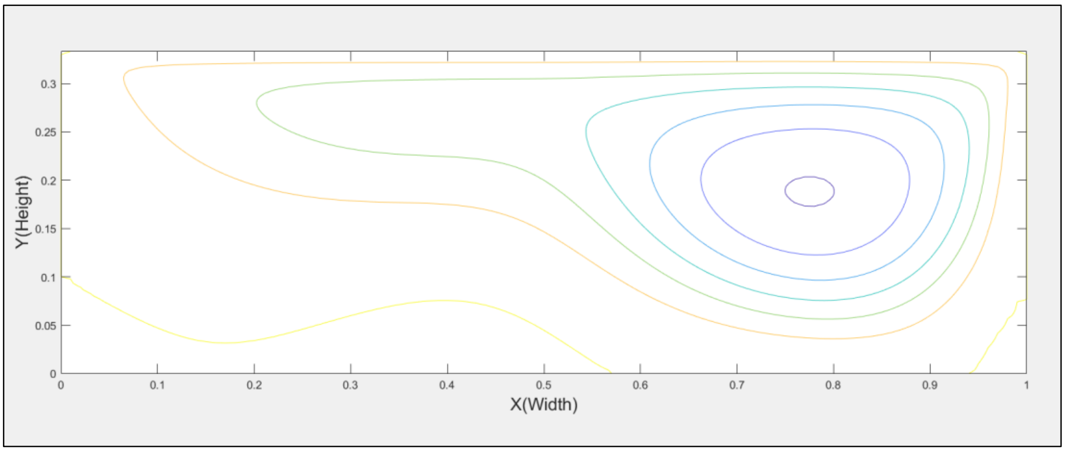

Fig. 10. *Simulation result for Re = 500.*

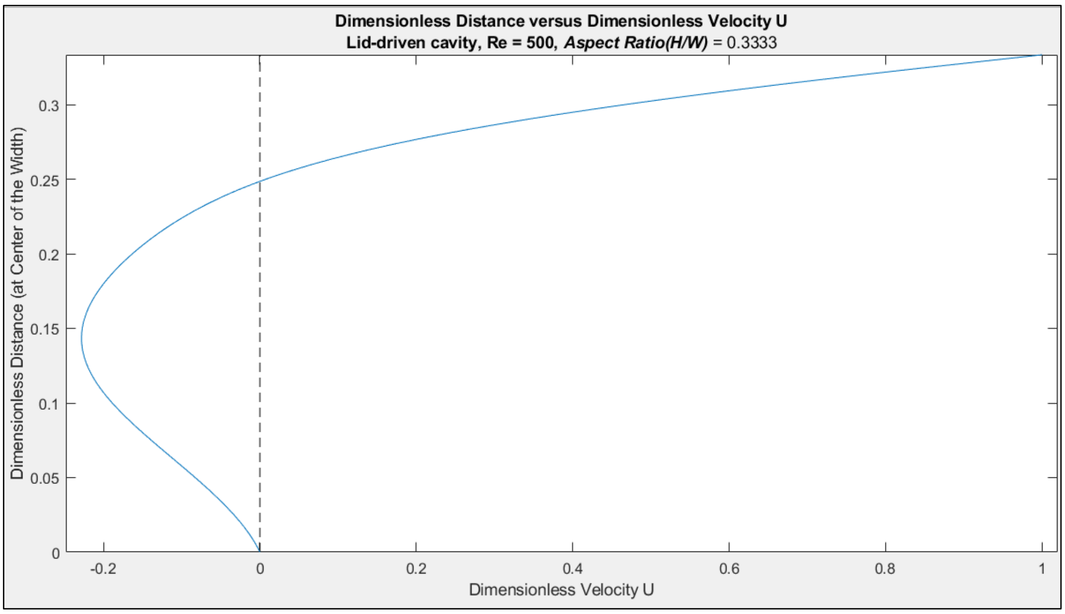

Fig. 11. *Simulation result for Re = 500.*

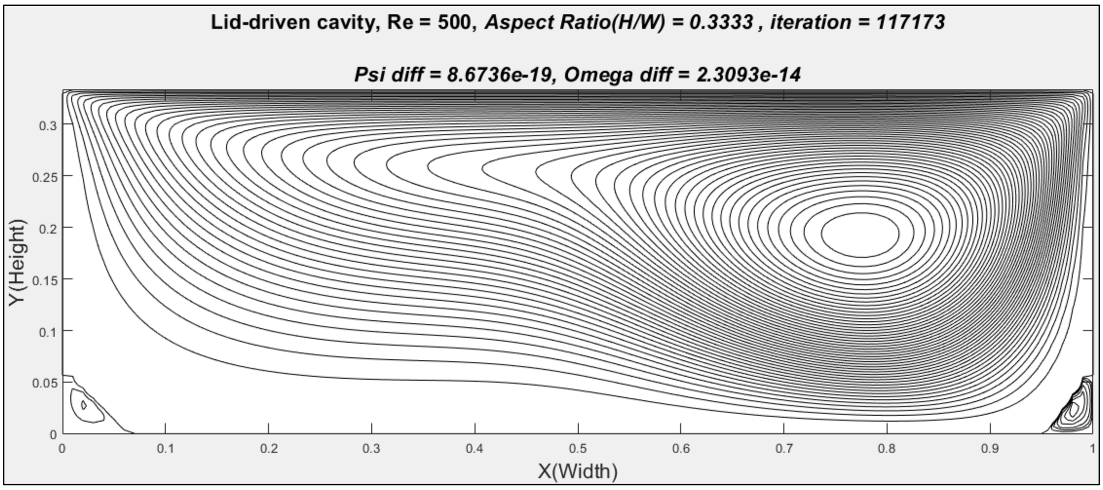

Fig. 12. *Simulation result for Re = 500.*

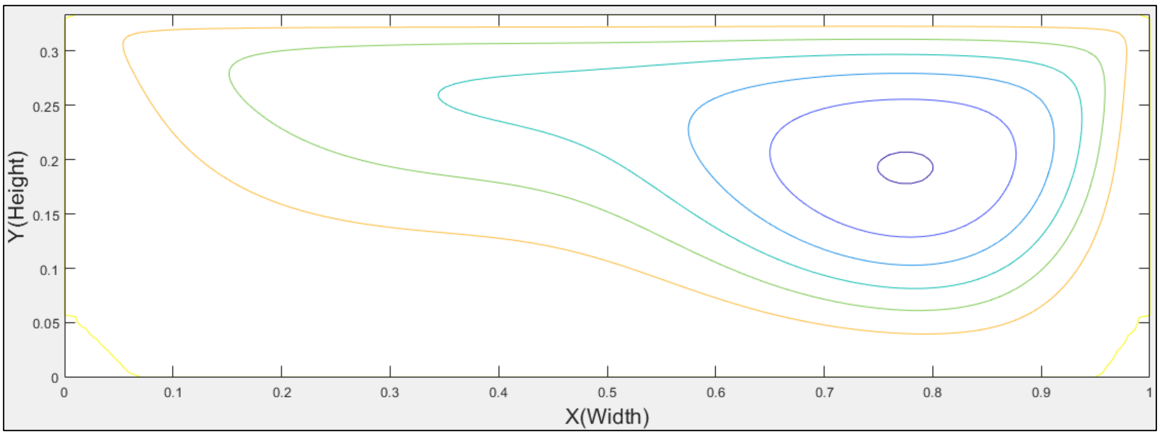

Fig. 13: *Simulation result for Re = 500.*

CONCLUSION

These equations show the velocity of the fluid particles at any point in the control 2D system. These equations cannot be solved arithmetically but have to be solved numerically. This has be done by the use of programing software MATLAB for the 1000, 750 and 500 values of Reynolds number.

REFERENCES

[1] Oztop HF. Combined convection heat transfer in a porous lid-driven enclosure due to heater with finite length. *Int Commun Heat Mass Transf*. 2006; 33(6): 772–779p.

[2] Yapici K, Karasozen B, Uludag Y. Finite volume simulation of viscoelastic laminar flow in a lid-driven cavity. *J Non-Newtonian Fluid Mech*. 2009; 164(1–3): 51–65p.

[3] Sheikholeslami M, Chamkha AJ. Flow and convective heat transfer of a ferro nanofluid in a double-sided lid-driven cavity with a wavy wall in the presence of a variable magnetic field. *Numer Heat Transf*. 2016; 69(10): 1186–1200p.

[4] Grillet AM, Yang B, Khomami B, Shaqfeh ESG. Modeling of viscoelastic lid driven cavity flow using finite element simulations. *J Non-Newtonian Fluid Mech*. 1999; 88(1–2): 99–131p.

[5] Billah MM, Rahman MM, Sharif UM, Rahim NA, Saidur R, Hasanuzzaman M. Numerical analysis of fluid flow due to mixed convection in a lid-driven cavity having a heated circular hollow cylinder. *Int Commun Heat Mass Transf.* 2011; 38(8): 1093–1103p.

[6] Freitas CJ, Street RL, Findikakis AN, Koseff JR. Numerical simulation of three-dimensional flow in a cavity. *Numer Methods Fluids*. 1985; 5(6): 561–575p.

[7] Alamsyah MNA, Simanjuntak CA, Bagustara BARH, Pradana WA, Gunawan PH. OpenMP analysis for lid driven cavity simulation using lattice Boltzmann method. *Conference: 2017 5th International Conference on Information and Communication Technology (ICoIC7)*. Malacca City, Malaysia. 2017, May 17–19.

[8] Lioua K, Oztop HF, Borjini MN, Al-Salem K. Second law analysis in a three-dimensional lid-driven cavity. *Int Commun Heat Mass Transf*. 2011; 38(10): 1376–1383p.

[9] Tsorng SJ, Capart H, Lai JS, Young DL. Three-dimensional tracking of the long-time trajectories of suspended particles in a lid-driven cavity flow. *Exper Fluids*. 2006; 40(2): 314–328p.

[10] Migeon C, Pineau G, Texier A. Three-dimensionality development inside standard parallelepipedic lid-driven cavities at Re = 1000. *J Fluid Struct*. 2003; 17(5): 717–738p.

[11] Rana A, Torrilhon M, Struchtrup H. A robust numerical method for the R13 equations of rarefied gas dynamics: application to lid driven cavity. *J Comput Phys*. 2013; 236: 169–186p.

[12] Mohamad AA, Viskanta R. Flow and heat transfer in a lid-driven cavity filled with a stably stratified fluid. *Appl Math Modell*. 1995; 19(8): 465–472p.

[13] Al-Amiri AA, Khanafer KM, Pop I. Numerical simulation of combined thermal and mass transport in a square lid-driven cavity. *Int J Therm Sci*. 2007; 46(7): 662–671p.

[14] Oztop HF. Combined convection heat transfer in a porous lid-driven enclosure due to heater with finite length. *Int Commun Heat Mass Transf*. 2006; 33(6): 772–779p.

[15] Moallemi MK, Jang KS. Prandtl number effects on laminar mixed

convection heat transfer in lid-driven cavity. *Int J Heat Mass Transf*. 1992; 35(8): 1881–1882p.

[16] Talebi F, Houshang A, Shahi MM. Numerical study of mixed convection flows in square lid-driven cavity utilizing nanofluid. *Int Commun Heat Mass Transf.* 2010; 37(1): 79–90p.

[17] Mansoura MA, Mohamed RA, Abd-El Aziz MM, Ahmed SE. Numerical simulation of mixed convection flows in a square lid-driven cavity partially heated from below using nanofluid. *Int Commun Heat Mass Transf.* 2010; 37(10): 1504–1512p.

Cite this Article: Venkatshivasaivivek Attaluri, Parth N. Solanki, Parth G. Patel, Jatin D. Gami, Nirvish P. Patel. CFD Applied to Fluid Flow Due to Motion of Lid Inside a Cavity. *International Journal of Thermal Energy and Application*. 2019; 1 (1): 30-43p.